Exact Tunneling Calculations[1,2]

Donald G. Truhlar[3] and Aron Kuppermann*

Contribution No. 4090 from the Arthur Amos Noyes Laboratory of Chemical Physics, California Institute of Technology, Pasadena, California 91109.
Received July 13, 1970

Abstract: The transition state theory of chemical reactions rests on the assumption that motion along a reaction path is separable from motion in directions transverse to it and that the latter are adiabatic, *i.e.*, that their quantum numbers are preserved as the reaction proceeds. This assumption requires that, in calculating quantum mechanical tunneling factors, the zero-point energy of the transverse motions be added to the potential energy along the reaction path to furnish an effective vibrationally adiabatic barrier which should be used in such calculations. All tunneling calculations reported so far have neglected such zero-point energy corrections or used unrealistic approximations for them, and most have also replaced the reaction barrier by approximate analytical fits for which transmission probabilities could be determined analytically. We have performed accurate quantum mechanical calculations by numerical techniques for the collinear exchange reactions of H + H_2 and D + D_2 and reached the following conclusions. (1) The results of transmission probability and tunneling factor calculations from Eckart potential fits to the potential energy barrier lead to substantial systematic errors, especially at low temperatures, and therefore should not be used. Further, correcting Shavitt's calculations to eliminate his numerical approximations brings the model he used into better agreement with experiment. (2) The results of calculations ignoring the zero-point energy of the transverse motion and its variation along the reaction path are dramatically different from the ones including it. Since the latter are in accord with the adiabatic derivation of transition state theory and the former are not, agreement of the latter with gas-phase experiments must be considered the result of fortuitous cancellations of errors and should not be construed as support for the assumption behind the theory.

In the past few years, noteworthy progress in the calculation of scattering probabilities and cross sections for single collisions of molecules and atoms has been made. Nevertheless, computations of tunneling factors to be used in the transition state theory of the rates of bimolecular gas phase chemical reactions have still usually been made using simplified models recommended mainly by their computational simplicity. In particular, the analytic solution for the scattering probabilities of a parabolic barrier[4] and Eckart's analytic solution for the scattering off a more realistic barrier[5] (which is now called the Eckart barrier) have been widely used. These barriers have fixed shapes and do not usually represent adequately the potential energy barrier for the particular reaction of interest; they lead at times to large errors.

In the present article we present a numerical method for calculating exact scattering probabilities (probabilities of tunneling through barriers and of nonclassical reflection of particles incident on a barrier which is too low to cause reflections according to classical mechanics) for general one-dimensional barriers. Then we apply this to realistic approximations to the potential barrier for the H + H_2 reaction.

Transition state theory[6-8] has been very important in the history, understanding, and practical applications of chemical kinetics (transition state theory is also called absolute reaction rate theory; a recent exposition of its application is given in Johnston's book[9]). An important part of transition state theory[9e] is the assumption that in the neighborhood of the transition state motion along the direction of a one-dimensional reaction path can be separated from the other motions of the reacting system and that a potential energy can be defined for motion along this path. This path can be extended to reach to reactants and products; we refer to the extended path, which is defined to be the minimum potential energy path from reactants to products, as the reaction path. The potential, as a function of the reaction coordinate s (distance along the reaction path), usually involves a barrier between reactants and products. This is the classical potential energy barrier $V(s)$. The effect of quantum mechanical tunneling through this barrier is included in the transmission coefficient (Boltzmann tunneling factor) which occurs in transition state theory. It usually has a very important effect on the calculated rate constants for light atoms or molecules. In the next section we review the work that has been done on calculating quantum mechanical transmission coefficients for transition state theory. Then we discuss what is the theoretically most justifiable way of calculating such coefficients. In the rest of the article, we present the results of numerical calculations done this way and show how they differ from those obtained by previous treatments.

Mortensen[10] has previously used numerical calculations of scattering probabilities from multidimensional barriers of general shape to calculate transmission coefficients for transition state theory. That is an extension of the usual transition state theory. Belford, *et al.*,[11] have calculated exact transmission functions of electrons through one-dimensional image barriers.

(1) This article is based on part of the thesis submitted by D. G. Truhlar in partial fulfillment of the requirements for the Ph.D. degree to the California Institute of Technology, Dec 1969.

(2) This work was supported in part by the United States Atomic Energy Commission, Report Code No. CALT-767P4-60.

(3) Department of Chemistry, University of Minnesota, Minneapolis, Minn. 55455.

(4) D. L. Hill and J. A. Wheeler, *Phys. Rev.*, **89**, 1140 (1953).

(5) C. Eckart, *ibid.*, **35**, 1303 (1930).

(6) H. Eyring, *J. Chem. Phys.*, **3**, 107 (1935).

(7) J. O. Hirschfelder, H. Eyring, and B. Topley, *ibid.*, **4**, 170 (1936).

(8) J. O. Hirschfelder and E. Wigner, *ibid.*, **7**, 616 (1939).

(9) H. S. Johnston, "Gas Phase Reaction Rate Theory," Ronald Press, New York, N. Y., 1966; (a) pp 133 ff, 190 ff, 230 ff; (b) p 235; (c) pp 193 ff; (d) Chapter 5 and Appendix C; (e) Chapter 8, sections D and E.

(10) E. M. Mortensen, *J. Chem. Phys.*, **48**, 4029 (1968).

(11) G. G. Belford, A. Kuppermann, and T. E. Phipps, *Phys. Rev.*, **128**, 524 (1962).

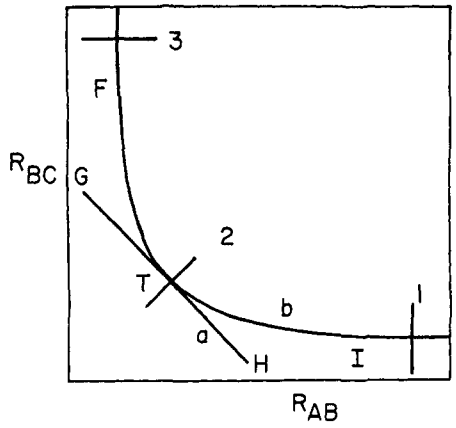

Figure 1. Two-dimensional orthogonal coordinate system for the linear reaction A + BC → AB + C. The path b from I to F is the path of minimum potential energy. T is the transition state. The path a from H to G corresponds to the asymmetric stretch normal-mode motion of the transition state and is tangential to the reaction path b at the saddle point T. Paths 1, 2, and 3 represent the transverse motion at several positions on path b. They are respectively the vibration of BC, the symmetric stretching vibration of ABC at the transition state, and the vibration of AB.

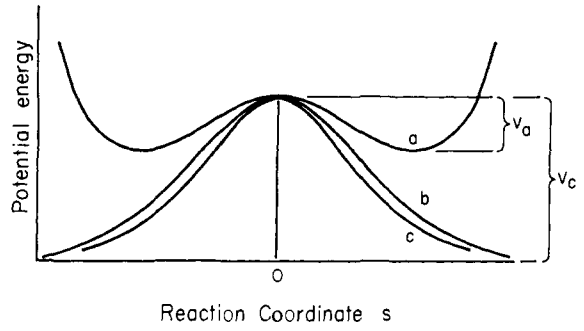

Figure 2. Barrier along various paths through the potential energy surface. Paths a and b are shown in Figure 1. Path c is the path of minimum potential energy in a transition state normal-mode coordinate system in which the cross term in the kinetic energy vanishes and the reduced mass is the same for motion in all directions (see ref 9d). This is a schematic figure for a general reaction with a symmetric surface.

Recently, Wyatt[12] and LeRoy, *et al.*,[13] have used similar methods for the transmission of particles through reactive-scattering-type one-dimensional barriers. Any of these methods could be used as an alternative to the one presented here. Child[14] and Connor[15] have considered semiclassical methods of calculating transmission functions for general one-dimensional barriers; their methods also provide useful alternatives for some cases.

Theory

Previous Treatments of Tunneling in One Mathematical Dimension. There are three basic approaches to the tunneling correction to transition state theory. The first is to consider it as a quantum mechanical correction to the (assumed separable) asymmetric-stretch rectilinear-coordinate normal-mode motion of the transition state.[9a,16-18] This procedure considers tunneling along path a (see Figures 1 and 2). The other two approaches consider tunneling along the reaction path b (or c). The second approach is to consider the tunneling as a correction to the (assumed separable) motion along this path in a modified transition state theory which treats all modes consistently including effects associated with the path's curvature.[19,20] Therefore, these curvilinear effects can be included consistently in the tunneling correction. This treatment, unlike the first approach, may be applicable even if the de Broglie wavelength for the motion along the potential surface is large compared to the size of the quadratic region of the saddlepoint region. The third approach (the one of most interest in this article) considers the tunneling correction as a transmission coefficient for the standard rectilinear-coordinate transition state theory (as given, *e.g.*, in ref 9), but may include in it any estimable effects due to the curvature of the reaction path or to the nonseparability of the multidimensional motion into motion along the reaction path and other motions. Based on these approaches, various models (with different criteria for choosing the parameters) and various numerical methods have been used. In this subsection we review the calculations that have been done by other authors. In the next subsection we critically discuss the models behind these calculations, and in the rest of the Theory section we discuss normal-mode coordinates and the numerical methods used in our calculations.

One of the usual methods to calculate a tunneling correction is to replace the classical potential energy barrier by a parabolic barrier which in one way or another approximates the true potential. The quantum mechanical transmission through this barrier can then be treated approximately[21,22] or by the exact analytical methods worked out by Bell[23] and others.[4,24-28] Many such applications have been made.[7,9b,16,17,19,22,24,29-38] Another model potential for which an exact analytical solution is possible is the one worked out by Eckart[5] and others.[16,18,39] For symmetric surfaces this barrier has two independent parameters. In applications, one has always been determined by the requirement that the curvature at the top of the barrier be equal to the curvature at the top of the classical potential energy barrier. Various procedures have been

(12) R. E. Wyatt, *J. Chem. Phys.*, **51**, 3489 (1969).
(13) R. J. LeRoy, K. A. Quickert, and D. J. LeRoy, *Trans. Faraday Soc.*, in press; University of Wisconsin Theoretical Chemistry Laboratory Technical Report No. WIS-TCI-384, 1970.
(14) M. S. Child, *Mol. Phys.*, **12**, 401 (1967).
(15) J. N. L. Connor, *ibid.*, **15**, 37 (1968).
(16) H. S. Johnston and D. Rapp, *J. Amer. Chem. Soc.*, **83**, 1 (1961).
(17) H. S. Johnston, *Advan. Chem. Phys.*, **3**, 131 (1961).
(18) H. S. Johnston and J. Heicklen, *J. Phys. Chem.*, **66**, 532 (1962).
(19) R. A. Marcus, *J. Chem. Phys.*, **41**, 610 (1964).
(20) R. A. Marcus, *ibid.*, **41**, 2614 (1964).
(21) E. P. Wigner, *Z. Phys. Chem., Abt. B*, **19**, 203 (1932).
(22) I. Shavitt, *J. Chem. Phys.*, **31**, 1359 (1959).
(23) R. P. Bell, *Trans. Faraday Soc.*, **55**, 1 (1959).
(24) J. Bigeleisen, F. S. Klein, R. E. Weston, and M. Wolfsberg, *J. Chem. Phys.*, **30**, 1340 (1959).
(25) T. E. Sharp and H. S. Johnston, *ibid.*, **37**, 1541 (1962).
(26) R. E. Weston, *ibid.*, **31**, 892 (1959).
(27) R. E. Weston, *Discuss. Faraday Soc.*, **44**, 163 (1968).
(28) R. A. Marcus, *ibid.*, **44**, 167 (1968).
(29) J. Bigeleisen, *J. Chem. Phys.*, **17**, 675 (1949).
(30) J. C. Polanyi, *ibid.*, **23**, 1505 (1955).
(31) I. Yasumori, *Bull. Chem. Soc. Jap.*, **32**, 1103, 1110 (1959).
(32) G. Chiltz, R. Eckling, P. Goldfinger, G. Huybrechts, H. S. Johnston, L. Meyers, and G. Verbeke, *J. Chem. Phys.*, **38**, 1053 (1963).
(33) R. B. Timmons and R. E. Weston, *ibid.*, **41**, 1654 (1964).
(34) F. Klein, A. Persky, and R. E. Weston, *ibid.*, **41**, 1799 (1964).
(35) D. J. LeRoy, B. A. Ridley, and K. A. Quickert, *Discuss. Faraday Soc.*, **44**, 92 (1968).
(36) I. Shavitt, *J. Chem. Phys.*, **49**, 4048 (1968).
(37) C. A. Parr, Ph.D. Thesis, the California Institute of Technology, Pasadena, Calif., 1968.
(38) W. R. Schulz and D. J. LeRoy, *J. Chem. Phys.*, **42**, 3869 (1965).
(39) H. Shin, *ibid.*, **39**, 2934 (1963).

used to assign the other parameter[9b,c,16-19,22,32,34-36,38,40-43] so as to make the Eckart barrier approximate in one form or another the correct classical potential energy barrier or the classical potential energy barrier along path a. In another procedure,[10,19] the second parameter is chosen to make the barrier height equal $V(0) + Z(0) - Z(-\infty)$, where $V(0)$ is the classical potential energy barrier height, $Z(0)$ is the harmonic approximation to the zero-point vibrational energy of the transition state, and $Z(-\infty)$ is the harmonic approximation to the reactant's zero-point vibrational energy. This is an attempt to include effects due to the nonseparability of the motion along the reaction path from the other motions of the system. Johnston and Rapp developed an approximation to the two-mathematical-dimension tunneling problem (hereafter denoted by 2-MD) which describes exchange reactions of the type $A + BC \rightarrow AB + C$, where the three atoms A, B, and C are confined to remain on a straight line. It consists in taking a Boltzmann average of Eckart tunneling corrections for several paths parallel to the a path in Figure 1.[16] It has been applied frequently.[9a,16,26,32,34,44,45] A version of this "2-MD" tunneling correction with a modified definition of the Eckart barriers has also been used.[42]

Transition State Theory. The transition state transmission coefficient is a quantum mechanical correction to the motion along the reaction path. It has been pointed out many times that the transition state theory results if one assumes a Boltzmann distribution of reactant energies and that all modes of motion of the system, except the separable motion along the reaction path, are adiabatic.[8,46-48] By this it is meant that the quantum numbers of these modes are conserved as motion along the reaction path proceeds. Let the reaction coordinate s vary from $-\infty$ for the reactant configuration to zero for the top of the barrier to $+\infty$ for the product configuration. The conserved total energy in the center-of-mass system is the sum $E = E_r(s) + E_\alpha(s)$, where E_r is the energy in the reaction mode and E_α is the energy in the other modes (the α or nonreactive modes). The reason that E_α is a function of s is that as we move along the reaction path, the potential energy function along the transverse directions varies, resulting in a change of the energies of the corresponding quantum states. Based on this adiabatic hypothesis, we calculate E_α along the path b (or c) (the path of minimum energy from reactants to products) to find its highest value $E_\alpha(0)$. Then, classically, reaction occurs for all $E_r(-\infty)$ such that $E_r(0) \geq 0$. Thus, as Hirschfelder and coworkers[8,46] and Marcus[47] have pointed out, the potential energy which is responsible for motion of the system along the reaction path is the quantum mechanical adiabatic energy of the nonreactive modes of motion of the system (*i.e.*, the energy $E_\alpha(s)$ of the system-minus-the-reaction mode). Although other interpretations of the transition state theory are possible, we believe this is the most reasonable one for discussing tunneling corrections. This interpretation disagrees with most of the calculations described in the previous section and especially with the statement that "the quantum correction for one supposedly separable coordinate does not constitute potential energy for the reaction coordinate."[9c] We consider this statement inconsistent with a proper interpretation of transition state theory. Marcus[47,49] emphasized the point of view adopted here and its importance in tunneling calculations (for the purposes of illustration Marcus did calculations[19,49] using the barrier height obtained from a vibrationally adiabatic treatment, but he approximated the force constant associated to motion along the reaction path by the force constant computed from the classical potential energy barrier instead of from the quantum mechanical adiabatic one described below).

For a linear atom–diatomic molecule collision A + BC, the only mode of motion besides the one along the reaction path (*i.e.*, the only nonreactive mode of motion) is successively a vibration of BC (when A and BC are far apart), a symmetric stretching vibration of ABC (at the transition state), and a vibration of AB (when AB and C are far apart) as indicated, respectively, by lines 1, 2, and 3 of Figure 1. Representing by t the corresponding transverse coordinate, the potential energy function $U_s(t)$ associated with this motion varies parametrically with the reaction coordinate in a continuous manner. For $s \rightarrow -\infty$ it is the potential energy for BC, for $s = 0$ it is the transition state symmetric stretch potential energy, and for $s \rightarrow +\infty$ it is the potential energy for AB. The potential energy for the reaction coordinate mode of motion is the classical potential energy (the one due to treating electronic motion quantum mechanically within the framework of the Born–Oppenheimer approximation and neglecting zero-point vibrational energy everywhere) plus the adiabatic vibrational energy in the nonreactive mode. Neglecting the change in energy in this mode associated with conservation of its quantum number and variation of $U_s(t)$ with s is treating it as *inactive* in Marcus' terminology.[50] We will call this neglect the conservation of vibrational energy (in the nonreactive mode) model. In it, the potential energy for motion along the reaction coordinate is determined entirely by the classical potential energy. It is expected to be a bad approximation for many reactions, including $H + H_2$. The model in which the quantum numbers of the nonreactive modes do not change is called the vibrationally adiabatic model and is, as mentioned above, the one from which transition state theory is most naturally derived.

For a collision in a plane or a collision in three-dimensional space we would also have to consider the adiabatic transformation of the rotations of the separated molecule and the orbital motion of A with respect to BC into bending vibrations and rotations as the reagents approach the transition state. For the planar $H + H_2$ case, the adiabatic energies of the rotations and bends have been worked out by Child[51] and Marcus.[52]

(40) J. H. Sullivan, *J. Chem. Phys.*, **39**, 3001 (1963).
(41) H. S. Johnston and P. Goldfinger, *ibid.*, **37**, 700 (1962).
(42) C. L. Kibby and R. E. Weston, Jr., *ibid.*, **49**, 4825 (1968).
(43) M. J. Kurylo, G. A. Hollinden, and R. B. Timmons, *ibid.*, **52**, 1773 (1970).
(44) H. Carmichael and H. S. Johnston, *ibid.*, **41**, 1975 (1964).
(45) R. L. Wilkins, *ibid.*, **42**, 806 (1965).
(46) M. A. Eliason and J. O. Hirschfelder, *ibid.*, **30**, 1426 (1959).
(47) R. A. Marcus, *ibid.*, **46**, 959 (1967).
(48) It was recently pointed out that this is true only at low temperature; see D. G. Truhlar, *ibid.*, **53**, 2041 (1970). However, this correction to the adiabatic derivation of transition state theory is not of interest in the present article.
(49) R. A. Marcus, *ibid.*, **45**, 4493 (1966).
(50) R. A. Marcus, *ibid.*, **20**, 359 (1952).
(51) M. S. Child, *Discuss. Faraday Soc.*, **44**, 68 (1968).
(52) R. A. Marcus, *J. Chem. Phys.*, **49**, 2617 (1968).

For the three-dimensional collision, an approximate consideration of this correlation has been worked out by Mortensen and Pitzer for the lowest rotational state of the separated molecule.[53] The adiabatic assumption is not expected to be as good an approximation for these rotations, orbital motions, and bending modes as it is for the vibrational transverse α mode of the collinear H + H_2 reaction.[52,54] In this article we make calculations only for linear collisions.

Normal-Mode Coordinates. For the computation of tunneling corrections to transition state theory, we must obtain the effective potential as a function of a reaction coordinate s. This coordinate is a distance measured along a reaction path. Rather than choosing the path b of minimum energy in R_{AB},R_{BC} configuration space, we take it as the path c of minimum energy in the transition state normal-mode coordinate space.

The transition state normal-mode coordinates for a linear A + BC reaction,[9d] which we shall denote by x_1 and x_2, are defined in such a way that the potential and kinetic energy functions are given, respectively, by

$$V = {}^1/_2 k_1 x_1^2 + {}^1/_2 k_2 x_2^2 + \text{higher order terms} \quad (1)$$

$$K = {}^1/_2 \mu_N(\dot{x}_1^2 + \dot{x}_2^2) \quad (2)$$

where $\dot{x}_i$ is the time derivative of x_i, k_1 is the symmetric stretch force constant, k_2 is a negative number (the asymmetric stretch force constant), and the coordinates of the saddle point are $x_1 = x_2 = 0$. This means that the effective reduced mass μ_N is the same for both normal modes; *i.e.*, it does not depend on the direction of motion in the two-dimensional space defined by this coordinate system. In addition, in the vicinity of the saddle point the potential and kinetic energy are simultaneously diagonal, and the motion is therefore separable in these coordinates. The normal-mode motion along x_2 (for $x_1 = 0$) represents the asymmetric stretch of the transition state and corresponds to the motion which leads to reaction (path a of Figure 1), whereas the motion along x_1 (for $x_2 = 0$) represents the symmetric stretch motion of the transition state (path 2 of Figure 1). Motion along x_2 is transverse (*i.e.*, orthogonal) to motion along x_1.

The separability, just mentioned, of the motion in the vicinity of the transition state is an important factor dictating the choice of the normal-mode coordinate system as the system in which the reaction path is to be defined for the purpose of determining the tunneling correction. Taking the saddle point as the common origin for measurement of both s and x_2, these two coordinates are almost equal near this point (where the reaction path is tangent to the x_2 axis), but differ elsewhere.

For the linear H + H_2 or D + D_2 system, with the saddle point at $R_{AB} = R_{BC} = R_0$, the normal-mode coordinate analysis furnishes

$$x_1 = (\sqrt{3}/2)(R_{AB} + R_{BC} - 2R_0) \quad (3)$$

$$x_2 = (1/2)(R_{BC} - R_{AB}) \quad (4)$$

$$\mu_N = (2/3)m_A \quad (5)$$

(53) E. M. Mortensen and K. S. Pitzer, *Chem. Soc., Spec. Publ.*, No. 16, 57 (1962).

(54) Reference 49 (see especially footnote 13); M. Karplus, *Discuss. Faraday Soc.*, 44, 91 (1968), including his footnotes 2 and 3; R. A. Marcus, *ibid.*, 44, 166 (1968).

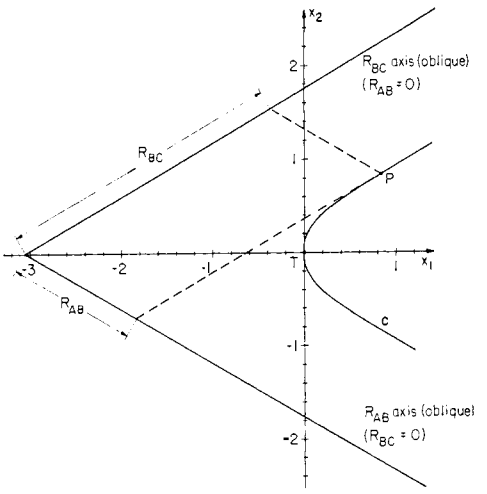

Figure 3. Reaction path c in normal-mode coordinate space x_1, x_2. The R_{AB}, R_{BC} values corresponding to an arbitrary point P on this path are indicated. The point T is the saddle point (classical transition state). Reaction path b is slightly different, but the difference would not show up clearly in this figure.

where m_A is the atomic mass. These are the normal mode coordinates used by Shavitt.[36]

Figure 3 indicates the reaction path c for the H + H_2 reaction in this normal-mode coordinate space. Reaction path b, although different, is close enough to path c for the differences not to show up clearly on the scale in which Figure 3 was drawn. The $R_{BC} = 0$ and $R_{AB} = 0$ lines can be considered as the R_{AB} and R_{BC} axis, respectively, in an oblique system of Cartesian coordinates for which the angle between the axes is 60°. This oblique system differs from the orthogonal R_{AB}, R_{BC} system of Figure 1 in the sense that the kinetic energy is diagonal in the former but not in the latter. It can be seen that the reaction paths have appreciable curvatures in the vicinity of the transition state. The potential energy surface from which these reaction paths are obtained is described in the Calculations section. The potential energy along the reaction path c as a function of the curvilinear distance s is considered to be a barrier along one Cartesian dimension s for the calculation of the tunneling coefficient; *i.e.*, we neglect reaction-path curvature in the stage of the calculation considered next.

Numerical Treatment of One-Dimensional Tunneling. The Schroedinger equation for one-dimensional motion along a reaction path in normal-coordinate space is, in any units for which $\hbar = 1$

$$\left[-\frac{1}{2\mu_N}\frac{d^2}{ds^2} + V(s) - E\right]\psi_k(s) = 0 \quad (6)$$

where $V(s)$ is an effective potential energy function, which is defined differently in different models, and E is the total energy of the system. The distance s along the reaction path in normal coordinate space is calculated by numerical line integration using a sufficiently fine grid (points about 0.06 a_0 apart) to achieve an accuracy of about 0.001 a_0. The index k labels degenerate solutions of equal energy. Of these solutions, a maximum of two can be linearly independent. To solve this equation for a given E we select a set of N evenly spaced mesh points s_i, $i = 1, 2, \ldots, N$, with $s_i < s_{i+1}$, and approximate the second derivative in eq

4 by central differences of order 2 at these points in the standard way.[55] This yields the set of N coupled linear equations

$$\sum_{j=1}^{N}(F^h_{ij} - \lambda\delta_{ij})\psi^h_{jk} = b_i \qquad i = 1, 2, \ldots, N \tag{7}$$

for the approximate values ψ^h_{jk} of the solutions $\psi_k(s_j)$ at the mesh points. In eq 7

$$\lambda = -2h^2E \tag{8}$$

$$h = s_{i+1} - s_i \tag{9}$$

$$F^h_{ij} = -2[(1/\mu_N) + h^2V(s_i)]\delta_{ij} + (1/\mu_N)(\delta_{i,j-1} + \delta_{i,j+1}) \tag{10}$$

$$b_i = (-1/\mu_N)[\psi_k(s_1 - h)\delta_{i1} + \psi_k(s_N + h)\delta_{iN}] \tag{11}$$

where δ_{ij} is the Kronecker delta. As $h \to 0$, the approximate solutions approach the exact ones, *i.e.*

$$\psi_k(s_j) = \lim_{h\to 0}\psi^h_k(s_j) \tag{12}$$

We choose $s_1 = -s_N$ and s_N to be large enough for $V(s_1)$ to be negligible, *i.e.*

$$V(s_N) \ll V(0) \tag{13}$$

$$V(s_1) \ll V(0) \tag{14}$$

where $V(0)$ is the height of the barrier.

The strategy of the method for finding solutions to eq 6 for a given E which corresponds as $s \to -\infty$ to an incident wave plus a superimposed reflected wave, and as $s \to \infty$ to a transmitted wave, is to first find two linearly independent solutions and impose these boundary conditions *a posteriori* on a linear combination of these two solutions. This is essentially an application to one-dimension barriers of the finite difference boundary value method of Diestler and McKoy.[56] We choose as the first independent solution the one which satisfies the arbitrary boundary conditions

$$\psi_1(s_1 - h) = 1 \tag{15}$$

$$\psi_1(s_N + h) = 0 \tag{16}$$

and as the second the one for which the boundary conditions are

$$\psi_1(s_1 - h) = 0 \tag{17}$$

$$\psi_2(s_N + h) = 1 \tag{18}$$

These choices are convenient in that they make these wave functions real everywhere. Since we are considering the case where the barrier is symmetrical about $s = 0$, we need not obtain the second solution by solving the set of eq 7 because we can obtain it from the first by reflection through $s = 0$. The asymptotic form of the solutions to the Schroedinger equation is

$$\psi_k(s) \underset{s\to\infty}{\sim} A_k e^{-ips} + \bar{A}_k e^{ips} \tag{19}$$

$$\psi_k(s) \underset{s\to-\infty}{\sim} \alpha_k e^{-ips} + \bar{\alpha}_k e^{ips} \tag{20}$$

where

$$p = (2\mu_N E)^{1/2} \tag{21}$$

(since $\hbar = 1$) and we do not use the bar to mean complex conjugate. We want to analyze the ψ^h_{jk} for large and small j (corresponding to large $|s|$) in the same way as $\psi_k(s)$. For large j, corresponding to the asymptotic region of the products, we have

$$A^h_k e^{-ips_i} + \bar{A}^h_k e^{ips_i} = \psi^h_{jk} \tag{22}$$

and

$$A^h_k e^{-ips_{i+}} + \bar{A}^h_k e^{ips_{i+l}} = \psi^h_{j+l,k} \tag{23}$$

where l is a small integer (usually equal to 1 or 2). Solving these equations for A^h_k and $\bar{A}^h_k$ gives

$$A^h_k = (\psi^h_{jk}e^{ips_{i+}} - \psi^h_{j+l,k}e^{ips_i})/D \tag{24}$$

$$\bar{A}^h_k = A^{h*}_k \tag{25}$$

$$D = 2i\sin(plh) \tag{26}$$

Equation 25 results from the fact that the ψ^h_{jk}'s are real. For small j, α^h_k and $\bar{\alpha}^h_k$ are given by similar equations. We consider the particle to be incident from the right of the barrier. The solution we seek has $A = 1$ and $\bar{\alpha} = 0$, *i.e.*

$$\psi(s) \underset{s\to\infty}{\sim} e^{-ips} + \bar{A}e^{ips}$$
$$\psi(s) \underset{s\to-\infty}{\sim} \alpha e^{-ips} \tag{27}$$

We can obtain this solution as a linear combination of any two linearly independent solutions. In terms of our approximate solutions we seek the linear combination of the independent solutions ψ^h_{j1} and ψ^h_{j2}

$$\psi^h_j = \sum_{k=1}^{2} C^h_k\psi^h_{jk} \tag{28}$$

for which the coefficients satisfy the boundary condition relations

$$\sum_{k=1}^{2} C^h_k A^h_k = 1 \tag{29}$$

$$\sum_{k=1}^{2} C^h_k \bar{\alpha}^h_k = 0 \tag{30}$$

Equations 29 and 30 can be written in matrix form as

$$\mathbf{A}^h\mathbf{C}^h = \mathbf{I}' \tag{31}$$

or

$$\begin{pmatrix} A^h_1 & A^h_2 \\ \bar{\alpha}^h_1 & \bar{\alpha}^h_2 \end{pmatrix}\begin{pmatrix} C^h_1 \\ C^h_2 \end{pmatrix} = \begin{pmatrix} 1 \\ 0 \end{pmatrix} \tag{32}$$

The probability of reflection from the barrier (R) and the probability of transmission across it (T) are given in terms of the asymptotic form of the solution ψ^h_j with scattering boundary conditions given by eq 29 and 30 by

$$R = \lim_{h\to 0}\left|\sum_{k=1}^{2} C^h_k\bar{A}^h_k\right|^2 = \left|\sum_{k=1}^{2} C_k\bar{A}_k\right|^2 \tag{33}$$

$$T = \lim_{h\to 0}\left|\sum_{k=1}^{2} C^h_k\alpha^h_k\right|^2 = \left|\sum_{k=1}^{2} C_k\alpha_k\right|^2 \tag{34}$$

For the case of symmetric potentials the only properties of the second linearly independent solution necessary

(55) L. Fox, "The Numerical Solution of Two-Point Boundary Value Problems in Ordinary Differential Equations," Clarendon Press, Oxford, 1957, pp 6–11.

(56) M. M. Pennell and L. M. Delves, *J. Math. Computation*, **15**, 243 (1961); D. J. Diestler and V. McKoy, *J. Chem. Phys.*, **48**, 2941, 2951 (1968); V. P. Gutschick, V. McKoy, and D. J. Diestler, *ibid.*, **52**, 4807 (1970).

for obtaining R and T are

$$A_2 = \bar{\alpha}_1 \quad (35)$$

$$\bar{A}_2 = \alpha_1 \quad (36)$$

$$\alpha_2 = \bar{A}_1 \quad (37)$$

$$\bar{\alpha}_2 = A_1 \quad (38)$$

The results can be obtained to an arbitrary accuracy without taking the limit in eq 33–34 by using small enough h. This procedure was programmed in FORTRAN IV for the Caltech IBM 7094 computer and the program was checked by computing R and T for the H + H_2 Eckart potential (which can also be obtained analytically as discussed above). In that case we could obtain R and T to an accuracy of 0.3% with $N = 100$ and 0.04% with $N = 400$. For the H_3 barriers we used $N = 400$ and $s_N = 4.0$ to 8.0 a_0. The computing time was about 1.0 sec per energy (at one energy we obtain one R and one T; the analysis of eq 24 and 25 was unnecessarily done at six pairs of s_i as a consistency check).

Calculations

An Accurate Analytic Potential Energy Surface for H_3. We may consider the H + H_2 reaction as proceeding in the ground electronic state with the nuclear motion determined by an effective potential calculated using the Born–Oppenheimer separation of electronic and nuclear motions. This potential has been calculated most accurately by Shavitt, Stevens, Minn, and Karplus (SSMK).[57] Their results confirm the conclusion of many earlier less accurate studies that the lowest energy reaction path for the H + H_2 reaction corresponds to a linear collision and that the highest potential energy that must be achieved along this minimum energy path (or reaction path) occurs for the configuration where the atoms are equally spaced on the line. The calculation predicts that this barrier height is 0.477 eV. Shavitt[36] estimated that the best guess of the real barrier height, as determined by comparing transition state theory to the rate experiments of Westenberg and de Haas[58] and others, is 0.424 eV. He suggested that the SSMK surface be modified by scaling the barrier by a factor (0.424/0.477) = 0.89 along the entire reaction path and that the curvatures at the barrier top (which is the transition state saddle point of the potential energy surface) in directions transverse to the reaction path be kept unchanged. This prescription determines the modified surface along the whole reaction path and over a small region close to it near the saddle point, but does not specify it elsewhere. We will assume that for linear collisions the transverse curvature along the entire reaction path is also unchanged.

Shavitt, *et al.*, fit their potential energy surface for linear collisions to an analytic function of the internuclear distances with 29 parameters.[57] This is a fit to the surface before scaling.

One-Dimensional Potential Energy Barriers, Including the Vibrationally Adiabatic Potential Energy Barrier. Shavitt, Stevens, Minn, and Karplus[57] computed the "minimum energy reaction path" b for the H + H_2 reaction in R_{AB},R_{BC} space. The coordinates of some points on their minimum energy path are given in Table VIII of ref 57. The energy as a function of distance along this path as plotted in the normal-coordinate space was used as the best approximation to the unscaled barrier by Shavitt.[36] However, the minimum-energy reaction path of interest in transition state theory is the path c of steepest descent in the *normal mode coordinate space* from the transition state (saddle point of the potential energy surface) to the reactants' configuration or, equivalently, the path of steepest ascent from the reactants' configuration to the transition state. This path c is different from path b of steepest descent and ascent in the R_{AB},R_{BC} space. We determined path c for the SSMK surface from the 29-parameter fit.[59] It is represented in Table I by pairs of R_{AB},R_{BC} values. The corresponding normal coordinate pairs x_1,x_2 can be obtained from eq 3 and 4. This path is plotted in Figure 3, and it did indeed turn out to be different from the one given in ref 57 and plotted in ref 36. The distances s were calculated by numerical line integration in normal-mode coordinate space along each of the reaction paths b and c, using the saddle point as the origin. The resulting effective one-dimensional barriers for motion (with reduced mass μ_N) along these reaction paths are given in Table II. The first one, for reaction path b, *will be called the Shavitt barrier.*[36] These barriers have already been scaled by 0.89. For convenience in calculating the tunneling correction, we performed a

Table I. Points on the Minimum-Energy Path c in Normal-Mode Coordinate Space for the H + H_2 Reaction[a]

SSMK surface	
R_{AB}	R_{BC}
1.765	1.765
1.784	1.745
1.808	1.720
1.867	1.671
1.925	1.623
2.045	1.555
2.111	1.525
2.162	1.505
2.235	1.483
2.299	1.467
2.409	1.448
2.479	1.439
2.547	1.432
2.614	1.426
2.681	1.421
2.744	1.417
2.822	1.414
2.900	1.411
2.965	1.409
3.031	1.407
3.093	1.406
3.153	1.405
3.212	1.404
3.300	1.403
3.518	1.402
3.582	1.401

[a] Distances are in bohrs.

(57) I. Shavitt, R. M. Stevens, F. L. Minn, and M. Karplus, *J. Chem. Phys.*, **48**, 2700 (1968); see corrections for linear configurations in footnote 13 of ref 36.

(58) A. A. Westenberg and N. de Haas, *ibid.*, 47, 1393 (1967).

(59) This path *cannot* be determined by fixing x_1 (or x_2) and finding the x_2 (or x_1) for which the potential energy is minimized. It must be found iteratively by minimizing the potential energy along the lines perpendicular to the reaction path. The whole calculation is performed in the x_1,x_2 space. Perpendicular lines in the R_{AB},R_{BC} space do not generally transform into perpendicular lines in the x_1,x_2 space.

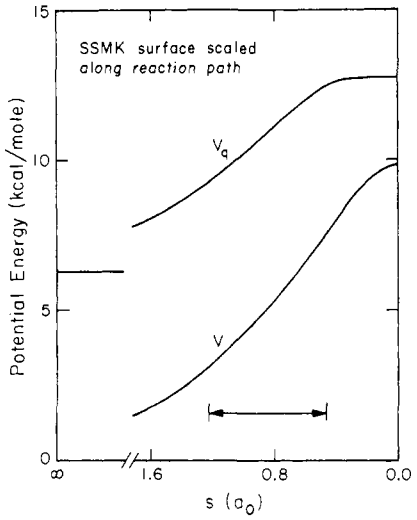

Figure 4. Potential energy barriers for the collinear H + H_2 as a function of distance s along the reaction path c (in the normal-coordinate space) from the saddle point of the surface: V, classical conservation-of-vibrational-energy barrier; V_q, quantum mechanical vibrationally adiabatic barrier. In the region indicated with the double-ended arrow the present V curve (reaction path c) is about 0.2 kcal/mol lower than Shavitt's barrier[36] (reaction path b).

least-squares fit of these barriers to expressions of the form

$$V(s) = b_1 \operatorname{sech}^2(b_3 s^2) + b_2 \exp(-b_4 s^2) + (B - b_1 - b_2) \exp(-4b_4 s^2) \quad (39)$$

where B is the barrier height $V(0)$ and the b_i's are given in Table II. The fits are illustrated in Table II, where

Table II. Potential Energy Barriers from the SSMK Surface as a Function of Distance from the Saddle Point. The Barriers Have Been Scaled by 0.89. In Both Cases, Distances Are Measured in the Transition State Normal-Mode Coordinate System

Path b[a]			Path c[c]		
s, a_0	V, eV	V_{fit},[b] eV	s, a_0	V, eV	V_{fit},[d] eV
0.000	0.424	0.424	0.000	0.424	0.424
0.104	0.417	0.419	0.044	0.422	0.423
0.160	0.407	0.411	0.099	0.417	0.418
0.226	0.393	0.399	0.152	0.408	0.410
0.301	0.375	0.381	0.257	0.383	0.387
0.385	0.353	0.357	0.314	0.367	0.371
0.478	0.327	0.329	0.358	0.355	0.358
0.585	0.297	0.296	0.424	0.336	0.337
0.717	0.261	0.257	0.482	0.319	0.319
0.852	0.225	0.221	0.583	0.289	0.287
0.990	0.191	0.188	0.649	0.270	0.267
1.131	0.159	0.158	0.714	0.252	0.249
1.332	0.120	0.122	0.843	0.217	0.215
1.542	0.087	0.090	0.904	0.202	0.201
1.768	0.061	0.063	1.056	0.167	0.168
1.998	0.041	0.042	1.186	0.141	0.142
2.274	0.024	0.024	1.306	0.120	0.121
2.500	0.019	0.014	1.424	0.101	0.102
			1.546	0.085	0.085
			1.606	0.078	0.077
			1.671	0.070	0.068

[a] References 36 and 57. This barrier was computed in normal-mode coordinate space using the minimum-energy path obtained from R_{AB},R_{BC} space. It is called the Shavitt barrier in this paper. [b] From eq 39 with b_1 = 0.0850 eV, b_2 = 0.2520 eV, b_3 = 0.25602 (bohr)$^{-2}$, b_4 = 0.89044 (bohr)$^{-2}$. [c] Present. This barrier was computed in normal-mode coordinate space using the minimum energy path from this space (given in Table I). [d] From eq 39 with b_1 = 0.1129 eV, b_2 = 0.2294 eV, b_3 = 0.30855 (bohr)$^{-2}$, b_4 = 1.11123 (bohr)$^{-2}$.

the numbers in the columns labeled V_{fit} are computed from eq 39.

We reexpressed the 29-parameter fit to the SSMK potential in normal coordinates and in this space computed its second derivative in the direction perpendicular to the reaction path c for points on this path. From this derivative at each of these points, we computed the force constant and zero-point energy of a harmonic oscillator of mass μ_N. These zero-point energies define a function $Z(s)$, which is the harmonic approximation to the zero-point energy of the motion transverse to the reaction coordinate. If $Z(s)$ is added to the potential energy function $V(s)$ along c (the "classical" or "conservation of vibrational energy" potential energy function) we get a "quantum" or "vibrationally adiabatic" barrier $V_q(s)$ for the case when the reagent diatomic molecule is initially in its ground vibrational state. According to the interpretation of transition state theory used by Hirschfelder, Wigner, Eliason, and Marcus[8,46,47] the one-dimensional transmission coefficient for ground-state reagent should be calculated using $V_q(s)$ and not $V(s)$. The transmission coefficient for a vibrationally excited reagent state α should be computed from the barrier obtained by adding to $V(s)$ the vibrational energy at position s of the transverse motion with the same quantum number α. Three $V_q(s)$ barriers for H_3 for the ground vibrational state have been determined recently by Wyatt.[12] His formulation of the problem is different from the present one and the case he treats is a collision in more dimensions.

The quantum barrier $V_q(s)$ for the ground vibrational state was computed for the classical potential energy function given in column 5 of Table II. The quantity $V_q(s) - Z(-\infty)$ is given in Table III, where $Z(-\infty)$ corresponds to the reagent configuration and is therefore the harmonic approximation to the zero-point

Table III. Quantum Barrier as a Function of the Distance from the Saddle Point for the Ground Vibrational State

s, a_0	$V_q - Z(-\infty)$,[a] eV	$[V_q - Z(-\infty)]_{fit}$,[b] eV
0.000	0.277	0.277
0.044	0.278	0.277
0.099	0.277	0.277
0.152	0.279	0.276
0.257	0.277	0.273
0.314	0.276	0.270
0.358	0.276	0.268
0.424	0.270	0.263
0.481	0.263	0.258
0.583	0.247	0.247
0.649	0.235	0.237
0.714	0.223	0.227
0.778	0.210	0.215
9.843	0.198	0.202
0.904	0.186	0.189
1.056	0.157	0.156
1.186	0.134	1.131
1.306	0.115	0.112
1.424	0.098	0.097
1.484	0.090	0.090
1.546	0.083	0.084
1.606	0.076	0.079
1.671	0.072	0.074

[a] V_q is the sum of the scaled $V(s)$ and the $Z(s)$ along the reaction path c in normal-mode coordinate space obtained from the SSMK surface. [b] From eq 39 with b_1 = 0.1099 eV, b_2 = 0.1050 eV, b_3 = 0.952810 (bohr)$^{-2}$, b_4 = 0.178496 (bohr)$^{-2}$, B = 0.2772 eV.

energy of the diatomic reagent. $V_q(s) - Z(-\infty)$ was fit to an expression of the form of the right-hand side of eq 39 by the least-squares method. The parameters of the fit and some values computed from it are also given in Table III.

Figure 4 illustrates the $V(s)$ and $V_q(s)$ barriers for the scaled SSMK surface for linear H_3. The $V_q(s)$ barrier for the strictly linear collisions is 0.277 eV high and is about 0.4 a_0 wider at the top than the classical barrier. Figure 4 shows that the $V_q(s)$ barrier does *not* have a shape which could be accurately approximated by an Eckart barrier.

One-dimensional scattering calculations off the two potentials $V(s)$ and $V_q(s)$ represent *two distinct models of the reaction.* Use of the classical potential $V(s)$ assumes *conservation of vibrational energy* (CVE) in the mode of motion transverse to the reaction path c. Use of the quantum potential $V_q(s)$ assumes *conservation of vibrational quantum number* (vibrational adiabaticity or VA) in that mode. The exact numerical solution of the scattering problem for these one-dimensional barriers will be discussed in the following subsections.

The simplest interpretation of the vibrational adiabaticity hypothesis is the one we use here, according to which the potential $V_q(s)$ is constructed by adding the local vibrational energy of the nonreactive mode to the classical potential energy along the minimum energy reaction path. This is not a strictly correct treatment because the coordinates are nonseparable, partly due to the curvilinear nature of the reaction path. One important effect of the curvature of the minimum energy reaction path and the nonseparability of the Schroedinger equation for the reaction coordinate and the transverse vibrational coordinate is a "centrifugal effect." This and other corrections to the simple scheme used here have been considered by Marcus[52,54,60] and Wyatt.[12]

Calculation of Boltzmann Tunneling Factors (Transmission Coefficients). The total energy of the reacting system A + BC in the center-of-mass coordinate system is, in transition state theory

$$\begin{aligned} E &= E_r + E^A{}_\alpha + E^{BC}{}_\alpha = E_r + E_\alpha \\ &= E^+{}_r + E^+{}_\alpha \end{aligned} \tag{40}$$

where E_r is the initial relative translational energy, $E^A{}_\alpha$ and $E^{BC}{}_\alpha$ are the initial internal energies of A and BC, respectively, for the system in state α (α represents the set of all quantum numbers for the separated subsystems), and $E^+{}_r$ is the energy available for motion along the reaction path at the transition state if the total internal energy in the other modes at the transition state is $E^+{}_\alpha$. E_α is the sum $E^A{}_\alpha + E^{BC}{}_\alpha$. Notice that $E^A{}_\alpha$, $E^{BC}{}_\alpha$, E_α, and $E^+{}_\alpha$ include not only the internal energies in the nonreactive modes of nuclear motion but also the change in electronic energy as a function of the change in nuclear coordinates. In the CVE model, $E^+{}_\alpha = E_\alpha + V(0)$, where $V(0)$ is the classical barrier height. In the VA model $E^+{}_\alpha$ is the classical barrier height plus the energy of the transverse (nonreactive) nuclear motion modes of the system at the transition state for the same quantum numbers α as for the separated reagent configuration; and therefore $E^+{}_\alpha \neq E_\alpha + V(0)$.

In either of these models the Boltzmann tunneling factor (or transmission coefficient) $\kappa(T)$ is defined as follows. Let $T(E_r,\alpha)$ be the exact one-mathematical-dimension (1-MD) transmission probability (or transmission function) for the reaction path barrier being considered (either CVE or VA) and for the reagents in internal state α approaching each other with initial relative kinetic energy E_r. The tunneling factor $\kappa_\alpha(T)$ for state α at temperature T is, by definition

$$\kappa_\alpha(T) = \frac{\int_{-\infty}^{\infty} T(E_r,\alpha) \exp(-E^+{}_r/kT)\mathrm{d}E^+{}_r}{\int_{-\infty}^{\infty} T^{cl}(E_r,\alpha) \exp(-E^+{}_r/kT)\mathrm{d}E^+{}_r} \tag{41}$$

where $T^{cl}(E_r,\alpha)$ is the classical 1-MD transmission probability defined by

$$\begin{aligned} T^{cl}(E_r,\alpha) &= 1 \text{ for } E^+{}_r \geq 0 \\ &= 0 \text{ for } E^+{}_r < 0 \end{aligned} \tag{42}$$

and E_r depends on $E^+{}_r$ according to eq 40. The overall tunneling factor for all states is then defined in the usual transition state theory (*cf.* ref 47) as the Boltzmann average over the nonreactive mode states of the transition state

$$\kappa(T) = \frac{\sum_\alpha \kappa_\alpha(T) \exp(-E^+{}_\alpha/kT)}{\sum_\alpha \exp(-E^+{}_\alpha/kT)} \tag{43}$$

Actually, the lower limits in the integrals in eq 41 should be the value of $E^+{}_r$ for which $E_r = 0$, since collisions with $E_r < 0$ do not exist. However, making by definition $T(E_r,\alpha)$ and $T^{cl}(E_r,\alpha)$ vanish for $E_r < 0$ permits using $-\infty$ for those lower limits. According to eq 41, therefore, the tunneling factor $\kappa_\alpha(T)$ is just the ratio of the averaged exact 1-MD quantum mechanical and classical transmission probabilities, where the weighting function is the Boltzmann factor for the energy $E^+{}_r$ available for reaction at the transition state. In view of eq 40, we can transform integration variables from $E^+{}_r$ to E_r and write eq 41, after cancellations of common factors in numerator and denominator, as

$$\kappa_\alpha(T) = \frac{\int_0^{\infty} T(E_r,\alpha) \exp(-E_r/kT)\mathrm{d}E_r}{\int_0^{\infty} T^{cl}(E_r,\alpha) \exp(-E_r/kT)\mathrm{d}E_r} \tag{44}$$

This indicates that in the averaging just mentioned, the Boltzmann factor appropriate for initial relative kinetic energy may be used. In eq 44 the energy conditions at the transition state play no special role other than their implicit involvement in the transmission probabilities. Using eq 42, eq 41 and 44 can be put in the forms

$$\kappa_\alpha(T) = (1/kT)\int_{-\infty}^{\infty} T(E_r,\alpha) \exp(-E^+{}_r/kT)\mathrm{d}E^+{}_r \tag{45}$$

and

$$\kappa_\alpha(T) = (e^{V_0/kT}/kT)\int_0^{\infty} T(E_r,\alpha) \exp(-E_r/kT)\mathrm{d}E_r \tag{46}$$

where E_r is related to $E^+{}_r$ by eq 40 and

$$V_0 = E^+{}_\alpha - E_\alpha \tag{47}$$

V_0 is the barrier height used to compute the difference in relative translational energies of the reagents and the

(60) R. A. Marcus, *J. Chem. Phys.*, 43, 2658 (1965).

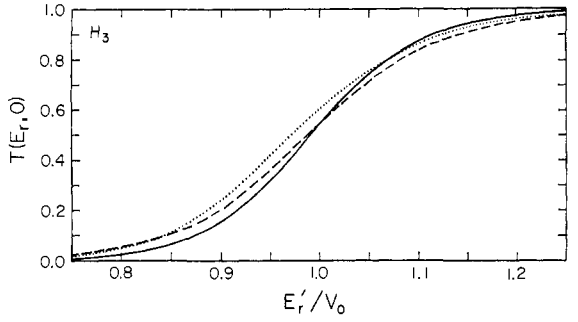

Figure 5. Transmission probability *vs.* reduced translational energy for H + H_2. V_0 is 0.424 eV for the three curves. For the dashed curve (usual Eckart barrier as described in text) and solid curve (barrier for reaction path c), E'_r is the initial relative kinetic energy E_r. For the dotted curve (Shavitt's false-bottom barrier of height 0.174 eV), E'_r is E_r plus the 0.250-eV difference between the height of the asymptotic region for this barrier and the correct one.

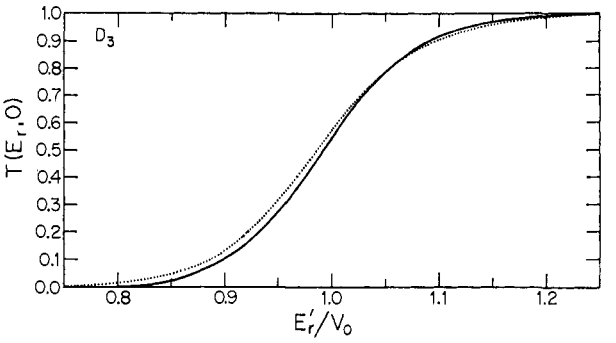

Figure 6. Transmission probability *vs.* reduced translational energy for D + D_2. Same abcissa and convention as for Figure 5.

system at the classical transition state; *i.e.*, it is the minimum initial relative translational energy necessary to go classically over the one-dimensional barrier being used.

For linear collisions H + H_2 and D + D_2 at temperatures at which only the ground electronic and vibrational states of the reagents are appreciably populated, $\kappa(T)$ is given by $\kappa_0(T)$ and is therefore

$$\kappa(T) = (1/kT)\int_{-\infty}^{\infty} T(E_r,0)\exp(-E^+_r/kT)\mathrm{d}E^+_r \quad (48)$$

where

$$E^+_r = E - E^+_0 = E_r + E_0 - E^+_0 \quad (49)$$

Shavitt has shown how the integral (48) can be recast as the sum of two finite range integrals which can be easily integrated.[61] He obtained accurate results (0.01%) using 200 points per integral. We have used his formula (eq 27 of ref 61) for the integrals but evaluated them using Gaussian integration. By using 21 points per integral (42 energy points in all) we were able to obtain accuracy usually *much* better than 1%.

Results

In his paper on correlation of experimental rate constants with theoretical data on the H_3 potential energy, Shavitt[36] used the CVE model where $V_0 = V(0)$. He represented the scaled SSMK classical potential energy barrier (the Shavitt barrier) by an Eckart potential having the correct curvature at its maximum and giving a good fit "over as much of its upper part as possible." He reasoned that the transmission probability is determined by the nature of the potential barrier in the region where $|s|$ is small, *i.e.*, close to the top of the barrier. This Eckart barrier has a height V_0 (as defined in eq 47) of only 0.174 eV (compared to V_0 = 0.424 eV for the Shavitt barrier) and therefore has a false bottom 0.250 eV above the correct one. He computed the corresponding tunneling factors which he considered to be the best available estimate of the exact ones for the Shavitt barrier. By using the numerical method of the present article we can compute the transmission functions for any potential barrier and we need not resort to fits with Eckart barriers. From these monoenergetic transmission functions we compute the tunneling factors as described above.

(61) I. Shavitt, University of Wisconsin Theoretical Chemistry Laboratory Technical Report No. WIS-AEC-23, 1959.

The exact transmission probabilities for some of the barriers discussed above are shown in Figure 5 for the H + H_2 and in Figure 6 for D + D_2. Figure 5 shows that the transmission probability curves for the reaction path c barrier (see Table II) and for the usual Eckart barrier (which has the same height and curvature at the top as the reaction path b barrier) cross at a translational energy about equal to the barrier height. However, the Eckart barrier is thinner and it is associated with greater quantum effects (more tunneling for energies below the barrier height and more reflection for energies above it). The transmission probability curve computed from Shavitt's false-bottom Eckart barrier does not cross the other curves at an energy equal to the barrier height energy. Thus his barrier does not appear to be a qualitatively correct approximation to an 0.424-eV barrier. It systematically predicts too much tunneling. Figure 6 shows that, as expected, the quantum effects are more important for H + H_2 than for D + D_2.

Columns 2 and 3 of Table IV show respectively the tunneling factors for the H + H_2 reaction computed using Shavitt's method (the 0.174-eV high Eckart barrier) and those we computed numerically for the exact Shavitt barrier (reaction path b, see Table II). Column 4 shows the tunneling factors we computed numerically for the accurate fit to the correct minimum energy path obtained from the scaled SSMK surface (see Table II). Columns 2–4 of Table V show the corresponding tunneling factors for the D + D_2 reaction.

For comparison with these attempts to do the problem more accurately than it is usually done, we also computed the tunneling factors using the usual Eckart barrier treatment (correct barrier height and curvature at top). The results are given in column 6 of Table IV and column 5 of Table V.

The tunneling factors in columns 2–4 and 6 in Table IV and columns 2–5 of Table V are based on the conservation-of-vibrational-energy approximation. We also computed tunneling factors using the vibrationally adiabatic quantum barrier presented earlier in this article. These tunneling factors are given in column 5 of Table IV. The transmission functions from which these tunneling factors are computed are compared with the corresponding CVE ones in Figure 7. The tunneling factors differ from each other much less than the transmission functions do because they are compared to the classical transmission functions for corresponding (different) barriers (see eq 44 and 46). If the two quantum

Table IV. Tunneling Factors for H + H_2 Reaction Computed for Five Barriers Discussed in the Text

T, °K	Shavitt Eckart barrier[a]	Shavitt barrier[b]	Correct scaled SSMK barrier[c]	VA barrier[d]	Eckart barrier[e]
150	502.30	*f*	*f*	4.67	*f*
200	45.00	57.39	83.48	1.81	666.25
250	13.13	11.25	14.74	1.35	44.10
300	6.49	5.09	6.21	1.19	11.59
350	4.17	3.26	3.80	1.11	5.61
400	3.11	2.47	2.79	1.07	3.63
450	2.53	2.05	2.26	1.04	2.74
500	2.17	1.80	1.95	1.03	2.25
550	1.93	1.63	1.75	1.02	1.96
600	1.77	1.52	1.61	1.01	1.76
650	1.65	1.43	1.51	1.00	1.62
700	1.56	1.37	1.44	1.00	1.52
750	1.48	1.32	1.38	0.99	1.44
800	1.43	1.28	1.33	0.99	1.39
850	1.38	1.25	1.29	0.99	1.34
900	1.34	1.22	1.26	0.99	1.30
950	1.31	1.20	1.23	0.99	1.27
1000	1.28	1.18	1.21	0.99	1.24
1050	1.26	1.16	1.19	0.99	1.22
1100	1.24	1.15	1.18	0.99	1.20
1150	1.22	1.14	1.16	0.99	1.18
1200	1.21	1.13	1.15	0.99	1.17
1250	1.19	1.12	1.14	0.99	1.15

[a] V_0 = 0.174 eV. Eckart barrier of ref 36 (false bottom). These tunneling factors are exactly the same if they are computed in the standard way for this barrier with V_0 = 0.174 eV as if they are computed for this barrier with the asymptotic floor raised and V_0 = 0.424 eV as discussed in the caption of Figure 5. We use the latter interpretation. [b] Numerical calculation for the exact Shavit barrier[36] (reaction path b, see the first three columns of Table II). [c] Numerical calculation for the normal-mode-coordinates reaction path barrier c (see Tables I and the last three columns of Table II). [d] Numerical calculation for the barrier of Table III. [e] V_0 = 0.424 eV. Usual Eckart barrier (correct height and curvature at top). [f] These results at 150°K are so large that they are probably not meaningful.

Table V. Tunneling Factors for D + D_2 Reaction Computed for Four Barriers Discussed in the Text

T, °K	Shavitt Eckart barrier[a]	Shavitt barrier[b]	Correct scaled SSMK barrier[c]	Eckart barrier[d]
150	61.17	60.74	104.91	
200	10.24	6.91	9.90	24.45
250	4.52	3.15	4.01	6.09
300	2.91	2.17	2.58	3.26
350	2.23	1.75	2.00	2.33
400	1.88	1.54	1.70	1.90
450	1.66	1.41	1.53	1.65
500	1.53	1.32	1.42	1.50
550	1.43	1.26	1.34	1.40
600	1.36	1.22	1.28	1.38
650	1.31	1.18	1.24	1.28
700	1.27	1.16	1.21	1.24
750	1.23	1.14	1.18	1.21
800	1.21	1.12	1.16	1.18
850	1.19	1.11	1.14	1.16
900	1.17	1.10	1.13	1.14
950	1.15	1.09	1.11	1.13
1000	1.14	1.08	1.10	1.12
1050	1.13	1.07	1.10	1.11
1100	1.12	1.07	1.09	1.10
1150	1.11	1.06	1.08	1.09
1200	1.10	1.06	1.08	1.08
1250	1.10	1.05	1.07	1.08

[a] V_0 = 0.174 eV. Eckart barrier of ref 36 (false bottom). [b] Numerical calculation for the exact Shavitt barrier[36] (reaction path b; see Table II). [c] Numerical calculation for the normal-mode-coordinates barrier (reaction path c; see Tables I and II). [d] V_0 = 0.424 eV. Eckart-barrier calculation the way it is usually done (this barrier has same height and curvature at top as the classical potential energy barrier for either path b or path c).

mechanical transmission functions were both compared to the classical transmission functions for the VA barrier (as the interpretation adopted here implies is correct) then the CVE tunneling factors would be much too small. The usual CVE treatment thus involves a theoretically unjustified renormalization to make the results reasonable.

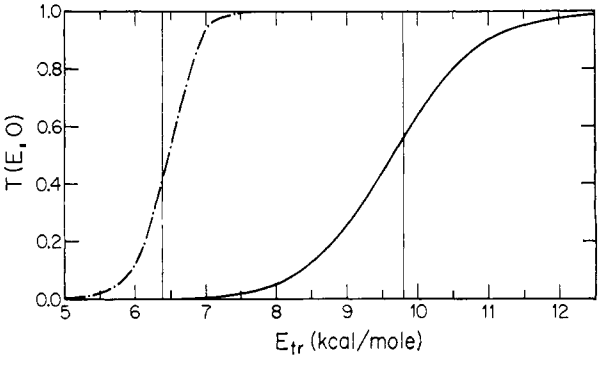

Figure 7. Transmission probability *vs.* translational energy for path c for H + H_2: —, CVE barrier; —·—·—, VA barrier. The vertical lines are drawn at energies corresponding to the heights of the respective barriers.

We also constructed another potential energy surface for linear H_3. This surface has the analytic form suggested by Wall and Porter.[62] It reduced to an accurate H_2 Morse curve at large H–H_2 separations. Three parameters for this surface are selected to give the scaled classical barrier height and scaled asymmetric stretch force constant suggested by Shavitt[36] and used above, and to make the transition state symmetric stretch force constant agree with that of the SSMK surface.[57] The one remaining parameter (*l* in the notation of Wall and Porter[58]) is selected to make the position of the mini-

(62) F. T. Wall and R. N. Porter, *J. Chem. Phys.*, 36, 3256 (1962).

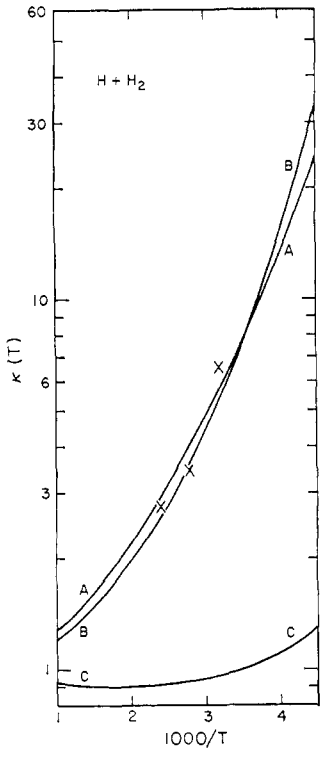

Figure 8. Tunneling factors for various barriers as a function of the reciprocal of the absolute temperature (°K): (A) Shavitt's false-bottom Eckart barrier, (B) correct scaled SSMK barrier (path c) in normal-mode coordinate space, (C) vibrationally adiabatic barrier. Curves A and B are for the CVE model and $V_0 = 0.424$ eV. Curve C is for the VA model and $V_0 = 0.277$ eV. ×'s represent the "correct harmonic oscillator partition function" results of LeRoy, Ridley, and Quickert;[35] these results are based on the CVE model. V_0 is not strictly defined in their method but is about 0.398 eV.

mum energy path agree well with that of the SSMK surface. Both the barrier from this surface and Shavitt's false-bottom Eckart barrier agree with the accurate barrier within 10% to about $s = 0.7$ a_0. At $s = 1.0$ a_0, the barrier from the Wall–Porter-type surface is about 35% low, and Shavitt's false-bottom Eckart barrier is about 40% high. Both approximate barriers differ appreciably from the accurate barrier for $s > 1.0$ a_0. However, the Wall–Porter-type surface barrier is accurate again for $s > 3$ a_0. Calculations in the CVE and VA models were carried out for this surface. The results were qualitatively similar to the ones already described (which used the scaled barrier from the 29-parameter fit to the SSMK surface). The transmission functions for the Wall–Porter-type surfaces barriers are being published separately.[63] For $T \geq 250$°K, the Boltzmann tunneling factors for the Wall–Porter-type surface VA barrier are smaller than those in column 5 of Table IV. For $T = 500$–600°K, the tunneling factors for this surface are a minimum and are 0.90. The tunneling factors for the Wall–Porter barrier in the CVE model agree with the tunneling factors in column 4 of Table IV within about 10% for $T > 400$°K and within 30% for $T \geq 300$°K. At lower temperatures, they are much higher because the barrier is too thin. In general, the 1-MD results for the two surfaces show similar trends; thus the Wall–Porter surface calibrated this way provides a scaled surface which is well defined in the whole R_{AB},R_{BC} space for linear collisions and is a good approximation to the scaled surface suggested but not constructed by Shavitt (see the subsection An Accurate Analytic Potential Energy Surface for H_3). This Wall–Porter analytic surface has also been used in calculations for H + H_2 and D + D_2 which treat accurately the 2-MD problem and therefore do not separate the motion along the reaction coordinate from the rest of the motion.[63]

The tunneling factors enter the transition state theory expression for the rate constant as a multiplicative factor. A plot of the logarithm of the tunneling factors *vs.* the reciprocal temperature gives curves whose ordinates are additive components of the logarithms of the rate constants. When the reaction rate constants are put on an Arrhenius plot (logarithm of reaction rate *vs.* the reciprocal of the temperature), the fact that the tunneling factors become large faster than linearly at high $1/T$ produces curvature on the Arrhenius plots. The curvature in the Arrhenius plots of experimental rates is usually interpreted as evidence of tunneling. Some of the tunneling factors in Table IV are plotted this way in Figure 8. The figure also includes for comparison the semiempirical tunneling factors obtained by LeRoy, Ridley, and Quickert[35] using their experimental data and their "correct harmonic oscillator partition function" method. (Their results were very model dependent and do *not* represent an experimental determination of the tunneling correction. No accurate experimental determination of this property exists.) The figure predicts that the tunneling correction gives a nonlinear contribution to the Arrhenius plot over a wide temperature range.

Discussion

The VA model is a consistent model for the linear encounter problem and will be discussed as such below. The linear VA model should not be applied in this form for a description of the three-dimensional reaction. This application and the application of a three-dimensional VA model to three-dimensional collisions are discussed at the very end of this section.

From an analysis of the results in Tables IV and V, the tunneling for the Shavitt barrier can be compared to the tunneling for Shavitt's Eckart approximation to it. Because the false bottom on his Eckart barrier (see the figure in ref 36) makes it too wide at energies much below the highest part, Shavitt's method underestimates the tunneling at low temperature (as expected) as can be seen from the results for $T \geq 200$°K in columns 2 and 3 of Table IV. However, evidently because its wrong behavior at large distances from the barrier top is equivalent to allowing the particle to surmount a large fraction of the barrier with zero reflection, the Shavitt Eckart barrier *overestimates* the tunneling due to the barrier over most of the experimentally accessible energy range, as indicated by the results at other temperatures in those two columns, as well as by the equivalent columns of Table V.

The standard Eckart barrier for the CVE model (column 6 of Table IV and column 5 of Table V) overestimates the tunneling as compared to the accurate treatment of the real barrier because the standard Eckart barrier is too thin for H_3. Because of the flat region in

(63) D. G. Truhlar and A. Kuppermann, *J. Chem. Phys.*, **52**, 3841 (1970), and unpublished work.

the VA barrier, it would not be a good approximation to fit an Eckart barrier to the H_3 VA barrier in the usual way.

The numerical result for the correct scaled SSMK barrier computed using the minimum energy path c for the normal-mode coordinate space must be considered the correct version of Shavitt's CVE model in which two aspects of the computations (the position of the minimum energy path and the evaluation of the transmission probabilities for the given barrier) are corrected. As can be seen from columns 2 and 4 of Tables IV and V, these tunneling factors are in good agreement with the Shavitt (false bottom) Eckart ones except at low temperatures where they are appreciably higher. As can be seen from curve A of Figure 8 and from Figures 3 and 4 of ref 36, these Shavitt Eckart results are in good agreement with experiment except at low temperatures ($T < 300$°K) where they are as much as 40% too low. Thus the new CVE results bring the theoretical and experimental results closer together at these low temperatures. The large errors in the tunneling factors for the Eckart approximations (columns 2 and 6 of Table IV and 2 and 5 of Table V) to the exact Shavitt barrier (column 3 of Tables IV and V), especially at low temperatures where the tunneling factor is most important, strongly suggest that these approximations should be avoided, since it is relatively simple to perform exact calculations, as described above. A similar conclusion has been reached recently and independently by LeRoy, Quickert, and LeRoy.[13]

The tunneling factors computed in the vibrationally adiabatic approximations are much different from those computed in the conservation-of-vibrational-energy approximations as dramatically illustrated by a comparison of columns 4 and 5 of Table IV and curves B and C of Figure 8. The tunneling factors computed for the wider vibrationally adiabatic $V_a(s)$ barrier are much smaller than those computed from the CVE $V(s)$ barriers—as expected. As seen from column 5 of Table IV, the tunneling factor for the VA treatment is slightly less than 1.0 for a wide temperature range, which means that there is more reflection for energies larger than the barrier height than tunneling for energies lower than the barrier height for a system with a Boltzmann distribution of relative translational energies. This last fact is a surprising result. It is the first time tunneling factors less than 1.0 have ever been reported.

Tunneling factors have generally been computed on the basis of linear collisions (see the Previous Treatments subsection above). The VA model we used to compute the tunneling factors is the correct model to use with transitions state theory for linear collisions (see ref 8, 46–47, and 64 and the Transition State Theory subsection above). Since the CVE results do not resemble the VA results, the usual treatment of tunneling appears to be theoretically unjustified for collisions in one dimension. It has not been fully tested for collisions in two or three dimensions. Thus, the significance in terms of molecular dynamics of any agreement of theory and experiment using the CVE models (such as reported two paragraphs above) is highly questionable. Including the adiabatic change in the rotational levels for collisions in two and three dimensions will make the VA barrier resemble the CVE barrier more closely again. This is because the rotational and relative orbital motions have no zero-point energy at large H–H_2 separations, but they become a rotation and a bend at the transition state. The bending vibration has a zero-point energy which raises the VA barrier for configurations close to the transition state. However, the amount of agreement of the VA and CVE barriers will then depend on summation and cancellation of at least two factors (decrease of vibrational energy of the symmetric stretching mode and increase of vibrational energy of the bending mode) and the interpretation will still not be straightforward. Further, the cancellation of errors may not be as complete for other reactions as it is for the H + H_2 one. In conclusion, use of the CVE barrier in transition state theory is an empirical model which has not been theoretically justified, and agreement between one-dimensional calculations using it and experiment (as shown in Figure 8) must be attributed to a fortuitous cancellation of compensating errors.

(64) R. A. Marcus, *J. Chem. Phys.*, 43, 1598 (1965).

Summary

Using numerical methods to solve for the exact transmission probabilities for general barriers has allowed us to separate the error in the quantum mechanical calculation of tunneling factors from the errors in the transition state theory. In this way, we corrected the numerical approximations in Shavitt's definitive transition state theory calculations for the usual tunneling model on H + H_2 and D + D_2. Further, we performed accurate tunneling calculations in the vibrational adiabatic model for the linear H + H_2 reaction. One of our conclusions is that much of the agreement between theory and experiment (ref 36 and above) obtained using the usual methods of calculating the tunneling (which are at least implicitly based on the assumption of inactive vibrational modes) is without firm theoretical foundation. Accurate tunneling calculations in the vibrational adiabatic model for the real H + H_2 reaction (*i.e.*, the H + H_2 reaction in three dimensions) will require first the determination of the vibrationally adiabatic potential surface for nonlinear collisions with nonzero impact parameter of H with rotating H_2. This VA surface has not yet been calculated. In a further study of the collinear H + H_2 reaction, we compare one-mathematical-dimension calculations of the type presented here with exact (two mathematical dimension) calculations.[63]

Acknowledgment. We are grateful to Dr. Isaiah Shavitt for helpful discussions.